



# Technical Report

**ISO/TR 23652**

## **Nanotechnologies — Considerations for radioisotope labelling methods of nanomaterials for performance evaluation**

*Nanotechnologies — Considérations relatives aux méthodes de  
marquage radio-isotopique des nanomatériaux pour l'évaluation  
des performances*

**First edition  
2024-06**

STANDARDSISO.COM : Click to view the full PDF of ISO/TR 23652:2024



**COPYRIGHT PROTECTED DOCUMENT**

© ISO 2024

All rights reserved. Unless otherwise specified, or required in the context of its implementation, no part of this publication may be reproduced or utilized otherwise in any form or by any means, electronic or mechanical, including photocopying, or posting on the internet or an intranet, without prior written permission. Permission can be requested from either ISO at the address below or ISO's member body in the country of the requester.

ISO copyright office  
CP 401 • Ch. de Blandonnet 8  
CH-1214 Vernier, Geneva  
Phone: +41 22 749 01 11  
Email: [copyright@iso.org](mailto:copyright@iso.org)  
Website: [www.iso.org](http://www.iso.org)

Published in Switzerland

# Contents

Page

<b>Foreword</b>	<b>iv</b>
<b>Introduction</b>	<b>v</b>
<b>1 Scope</b>	<b>1</b>
<b>2 Normative references</b>	<b>1</b>
<b>3 Terms and definitions</b>	<b>1</b>
<b>4 Abbreviated terms</b>	<b>2</b>
<b>5 Biodistribution study and radioisotopes</b>	<b>3</b>
5.1 Biodistribution study	3
5.2 Radioisotopes	3
<b>6 Radioisotope labelling methods for nanomaterials</b>	<b>4</b>
6.1 General	4
6.2 Pre- and post-surface labelling method	6
6.3 Chelating agent-based labelling	6
6.4 Chelating agent-free radioisotope labelling method	8
6.4.1 General	8
6.4.2 Radioactive-plus-non-radioactive precursors	8
6.4.3 Specific trapping	8
6.4.4 Cation exchange	9
6.4.5 Neutron or proton beam activation	10
6.5 Dual radioisotope labelling	10
6.6 Choice of radioisotopes	11
6.7 Production of radioisotopes	11
6.7.1 General	11
6.7.2 Cyclotron-produced radioisotopes	12
6.7.3 Reactor-produced radioisotopes	12
6.7.4 Generator-produced radioisotopes	13
6.8 Chelating agent and the matched pair for radioisotope	13
<b>7 The stability of radioisotope-labelled nanomaterials</b>	<b>14</b>
<b>8 Advantages and disadvantages of radioisotope labelling method</b>	<b>15</b>
<b>Annex A (informative) Representative radioisotopes used for nanomaterial labelling</b>	<b>16</b>
<b>Annex B (informative) Advantages and disadvantages of radioisotope labelling methods for nanomaterials</b>	<b>17</b>
<b>Bibliography</b>	<b>18</b>

## Foreword

ISO (the International Organization for Standardization) is a worldwide federation of national standards bodies (ISO member bodies). The work of preparing International Standards is normally carried out through ISO technical committees. Each member body interested in a subject for which a technical committee has been established has the right to be represented on that committee. International organizations, governmental and non-governmental, in liaison with ISO, also take part in the work. ISO collaborates closely with the International Electrotechnical Commission (IEC) on all matters of electrotechnical standardization.

The procedures used to develop this document and those intended for its further maintenance are described in the ISO/IEC Directives, Part 1. In particular, the different approval criteria needed for the different types of ISO document should be noted. This document was drafted in accordance with the editorial rules of the ISO/IEC Directives, Part 2 (see [www.iso.org/directives](http://www.iso.org/directives)).

ISO draws attention to the possibility that the implementation of this document may involve the use of (a) patent(s). ISO takes no position concerning the evidence, validity or applicability of any claimed patent rights in respect thereof. As of the date of publication of this document, ISO had not received notice of (a) patent(s) which may be required to implement this document. However, implementers are cautioned that this may not represent the latest information, which may be obtained from the patent database available at [www.iso.org/patents](http://www.iso.org/patents). ISO shall not be held responsible for identifying any or all such patent rights.

Any trade name used in this document is information given for the convenience of users and does not constitute an endorsement.

For an explanation of the voluntary nature of standards, the meaning of ISO specific terms and expressions related to conformity assessment, as well as information about ISO's adherence to the World Trade Organization (WTO) principles in the Technical Barriers to Trade (TBT), see [www.iso.org/iso/foreword.html](http://www.iso.org/iso/foreword.html).

This document was prepared by Technical Committee ISO/TC 229, *Nanotechnologies*.

Any feedback or questions on this document should be directed to the user's national standards body. A complete listing of these bodies can be found at [www.iso.org/members.html](http://www.iso.org/members.html).

## Introduction

Prior to the clinical trials of nanomaterials intended for use in human medicine, their *in vivo* behaviour has been evaluated in animal experiments. Several quantitative methods for assessing the biodistribution of nanomaterials have been developed. Among these methods, the biodistribution of radioisotope-labelled nanomaterials provides quantitative information on their distribution throughout the entire body.

The use of radioisotope-labelled nanomaterials for biodistribution studies is a well-established method for understanding the pharmacokinetics or toxicokinetics of nanomaterials *in vivo*. These methods assume that the distribution pattern of nanomaterials and radioisotope-labelled nanomaterials will be similar or nearly identical *in vivo*.

Radioisotope labelling of nanomaterials can be accomplished using a wide variety of radionuclides and associated labelling methods. However, for nanomaterials used for medicinal purposes, there are only a few matching pairs of nanomaterial and radioisotope labelling method that ensure the *in vivo* integrity of the radioisotope-labelled nanomaterial. Failure to identify and apply matching pairs of nanomaterial and radioisotope labelling method in studies preceding the clinical trial phase can lead to experimental data on biodistribution in which the nanomaterial and radio-label separate during the experiment. This in turn can result in a large number of nanomaterials or nano-drugs failing in the clinical trial phase.

STANDARDSISO.COM : Click to view the full PDF of ISO/TR 23652:2024

STANDARDSISO.COM : Click to view the full PDF of ISO/TR 23652:2024

# Nanotechnologies — Considerations for radioisotope labelling methods of nanomaterials for performance evaluation

## 1 Scope

This document provides:

- a) a review of radioisotope labelling methods that can be used for nanomaterials;
- b) the advantages and disadvantages of each radioisotope labelling method;
- c) information on the selection of a matched pair of nanomaterial and radioisotope labelling method to ensure the in vivo integrity of radioisotope-labelled nanomaterials<sup>1</sup> or the stability of their performance.

## 2 Normative references

The following documents are referred to in the text in such a way that some or all of their content constitutes requirements of this document. For dated references, only the edition cited applies. For undated references, the latest edition of the referenced document (including any amendments) applies.

ISO 80004-1, *Nanotechnologies — Vocabulary — Part 1: Core vocabulary*

ISO/TS 80004-8, *Nanotechnologies — Vocabulary — Part 8: Nanomanufacturing processes*

## 3 Terms and definitions

For the purposes of this document, the terms and definitions given in ISO 80004-1, ISO/TS 80004-8 and the following apply.

ISO and IEC maintain terminology databases for use in standardization at the following addresses:

- ISO Online browsing platform: available at <https://www.iso.org/obp>
- IEC Electropedia: available at <https://www.electropedia.org/>

### 3.1

#### **nanoscale**

length range approximately from 1 nm to 100 nm

[SOURCE: ISO 80004-1:2023, 3.1.1]

### 3.2

#### **nanomaterial**

material with any external dimension in the *nanoscale* (3.1) or having internal structure or surface structure in the nanoscale

[SOURCE: ISO 80004-1:2023, 3.1.4, modified — Notes have been removed.]

**3.3****nanoparticle**

nano-object with all external dimensions in the *nanoscale* (3.1)

Note 1 to entry: If the dimensions differ significantly (typically by more than three times), terms such as nanofibre or nanoplate are preferred to the term nanoparticle.

[SOURCE: ISO/TS 80004-1:2023, 3.3.4]

**3.4****radioisotope**

unstable isotope of an element that decays or disintegrates spontaneously, emitting ionizing radiation that can be alpha particles, beta particles and/or gamma rays

Note 1 to entry: Approximately 5 000 natural and artificial radioisotopes have been identified.

[SOURCE: ISO 19461-1:2018, 3.9, modified — "that can be alpha particles, beta particles and/or gamma rays" has been added to the definition.]

**3.5****biodistribution**

technique used to monitor the movement and distribution of specific radiolabelled *nanomaterials* (3.2) within an experimental animal or human subject

**3.6****chelating agent**

substance having a molecular structure embodying several electron-donor groups which render it capable of combining with metallic ions by chelation

[SOURCE: ISO 862:1984, 81]

**3.7****specific activity**

total radioactivity of the sample divided by its mass

Note 1 to entry: Specific activity is expressed in Bq/g.

[SOURCE: ISO 3925:2014, 3.4, modified — In the term, "activity" has been changed to "radioactivity"; Note 1 to entry has been added.]

**4 Abbreviated terms**

BFC	bifunctional chelating agent
NP	nanoparticle
TATE	1,4,8,11- tetraazacyclotetradecane-1,4,8,11-tetraacetic acid
CB-TE2A	4,11-bis(carboxymethyl)-1,4,8,11-tetraazabicyclo[6.6.2]hexadecane
NOTA	1,4,7-triazacyclononane-1,4,7-triacetic acid
DOTA	1,4,7,10-tetraazacyclododecane- 1,4,7,10-tetraaceticacid
DFO	desferrioxamine
PET	positron emission tomography
SPECT	single photon emission computed tomography



## 5 Biodistribution study and radioisotopes

### 5.1 Biodistribution study

Biodistribution studies involve tracing the movement of materials of interest in an experimental animal or human subject.<sup>[1][2]</sup> For any medicinal product intended for human administration, whether in experimental conditions during clinical trials or as an established treatment after approval by regulatory authorities, extensive information is generated in anticipation of human administration to understand the potential benefits and risks, as well as to anticipate and estimate the potential benefit-risk ratio profile.<sup>[3]</sup> The biodistribution of radiolabelled nanomaterials can be assessed using various methods, including image quantification, tissue radioactivity measurement, or autoradiography.

Image-based biodistribution can be done by tracking the distribution of radiolabelled nanomaterials of interest in an experimental animal or human subject using imaging techniques such as positron emission tomography (PET), single-photon emission computed tomography (SPECT). This approach allows researchers to visualize and quantify the spatial and temporal distribution of the nanomaterials of interest in vivo, enabling them to better understand their pharmacokinetics and pharmacodynamics<sup>[4]</sup>. Tissue-based biodistribution is a preclinical research technique that involves the analysis of the distribution and accumulation of radiolabelled nanomaterials in different tissues and organs of an animal or animal model. This technique provides information on the pharmacokinetics and pharmacodynamics of nanomaterials, which can include its absorption, distribution, metabolism and elimination (ADME) in different organs and tissues.<sup>[5]</sup> To perform a tissue-based biodistribution study, animals are typically treated with radiolabelled nanomaterials. After a predetermined time, animals are sacrificed, and different tissues and organs are collected and analysed for the presence and concentration of the drug. Whole-body slices can be made to visualize the distribution of radioactivity in different organs and tissues using autoradiography. This technique involves exposing the sliced tissue sections to a photographic film or imaging plate, which detects the radioactive emissions and generates an image that can be analysed to determine the distribution of the radiolabelled nanomaterial. Autoradiography is a widely used technique in preclinical research for evaluating the biodistribution of radiolabelled nanomaterials, and it can provide valuable insights into how the drug or nanomaterial is distributed throughout the body<sup>[6]</sup>.

The administration route of nanomaterials, such as intravenous, inhalational, intratracheal, oral, or intraperitoneal administration, can also be considered based on the intended clinical application. The administration route is an important consideration when assessing the biodistribution of nanomaterials since different routes can lead to distinct distribution patterns and pharmacokinetic profiles. Therefore, researchers carefully select the appropriate method and administration route to obtain accurate and reliable results.

### 5.2 Radioisotopes

Radioisotopes are isotopes that emit radiation and are commonly used for the diagnosis and treatment of various human diseases. Diagnostic purposes make up about 90 % of radioisotope usage, while therapeutic treatment makes up the remaining 10 %. Radioisotopes are labelled onto disease-targeting molecules, which are then administered and targeted to specific organs or tissues through specific mechanisms. The information from the radioisotopes is then collected and reconstructed by an imaging instrument to provide information about disease localization and specific biological processes. Typically, diagnostic radioisotopes are preferred for biodistribution studies because they have longer penetration depth and lower toxicity than therapeutic radioisotopes.  $\gamma$  or  $\beta^+$  emitters are commonly used for this purpose.<sup>[7]</sup>

The ability of  $\gamma$  rays to penetrate through the body depends on their energy, with higher energy leading to higher penetration ratios. However, excessively high energy can decrease the detector's sensitivity and resolution. As such, moderate-energy  $\gamma$  rays (between 30 keV and 300 keV) are optimal for  $\gamma$  camera or SPECT imaging.<sup>[8][9]</sup>  $\beta^+$  particles can create two  $\gamma$  photons (each with an energy of 511 keV) via an annihilation reaction, making them suitable for PET imaging. The range of a positron is influenced by its kinetic energy, with lower kinetic energy leading to better imaging quality.<sup>[10]</sup> When labelling nanomaterials with radioisotopes, the physical half-life is also a critical factor to be considered because specific nanomaterials have varying biological half-lives.

## 6 Radioisotope labelling methods for nanomaterials

### 6.1 General

The methods for radioisotope labelling and imaging of nanomaterials are crucial for various biomedical applications. Two common approaches for radioisotope labelling are chelating agent-based ([Figure 1](#), a) and chelating agent-free ([Figure 1](#), b to e) methods, as shown in the figure below.

Chelating agent-based methods involve the attachment of a chelating agent to the surface of the nanomaterial, which then binds to a radioisotope. This approach provides stable binding and high labelling efficiency. However, it can also result in the modification of the nanomaterial's properties and potential toxicity.

Chelating agent-free methods involve the direct binding of the radioisotope to the nanomaterial surface without the use of a chelating agent. This approach preserves the nanomaterial's properties and reduces potential toxicity. However, it can have lower labelling efficiency and stability.

Overall, the choice of labelling method depends on the specific application and desired properties of the labelled nanomaterial.<sup>[11]</sup>

STANDARDSISO.COM : Click to view the full PDF of ISO/TR 23652:2024

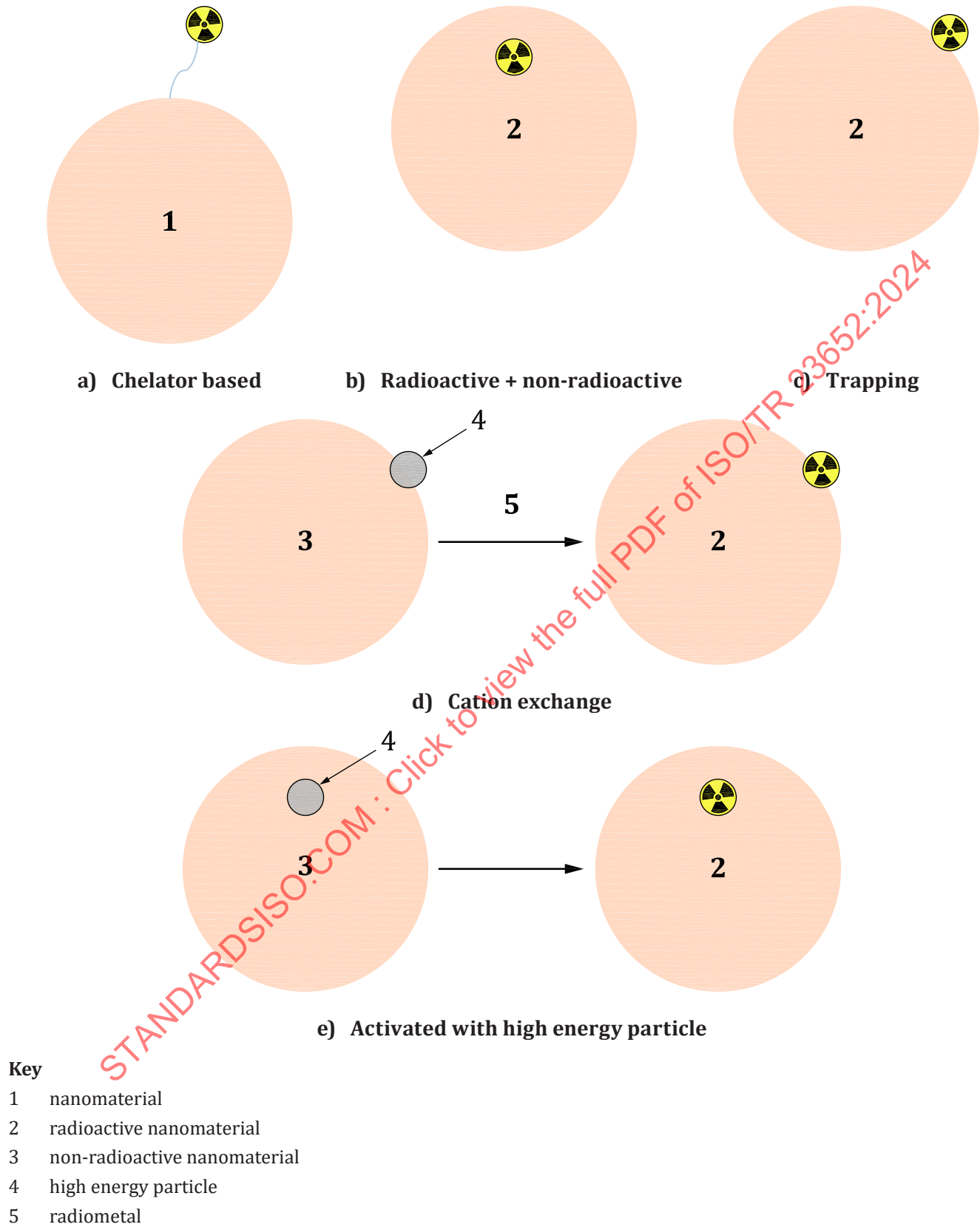
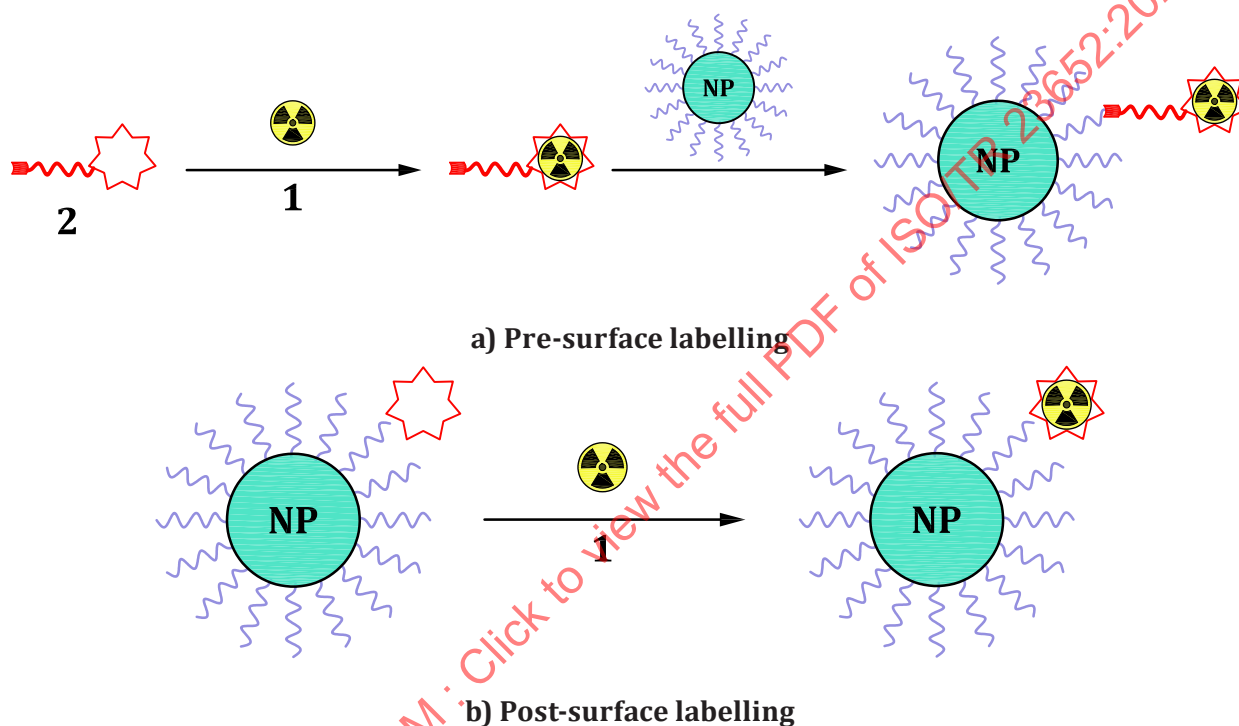


Figure 1 — Radioisotope labelling methods for nanomaterials

## 6.2 Pre- and post-surface labelling method

There are two approaches to radioisotope labelling of surface-modified nanomaterials, pre- and post-surface labelling methods, as shown in Figure 2.<sup>[12]</sup> The pre-surface-labelling method can be used for nanomaterials that contain conjugation motifs on the surface, while the post-surface-labelling method can be used for chelating agents on the surface. The radioisotope labelling procedure can involve harsh reaction conditions, such as high/low pH, high temperature and/or the use of reducing or oxidizing agents. Therefore, the pre-labelling method is a better choice for nanomaterials that are acid/base or high-temperature labile and cannot meet such radioisotope labelling conditions directly.

Click chemistry, which was coined by the K. Barry Sharpless group in 2001, is a type of chemical reaction that can be easily and rapidly achieved.<sup>[13]</sup> It might be the best tool for the pre-surface labelling method. Clickable nanomaterials can be labelled with radioisotope-labelled bifunctional chelating agents under aqueous conditions and pH 7,4 at room temperature.



### Key

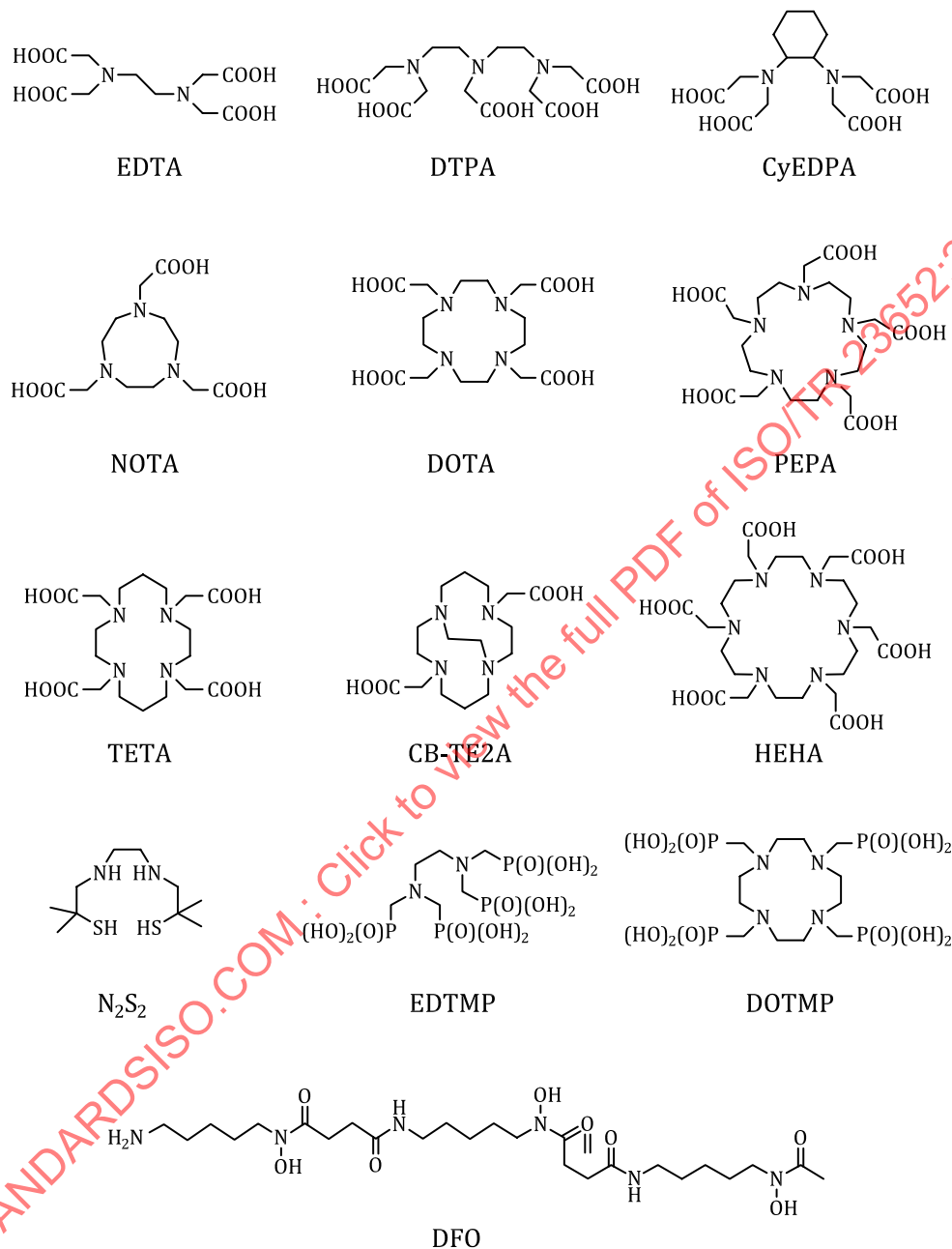
- 1 radioisotope
- 2 bifunctional chelating agent

Figure 2 — Schematic procedure of the pre- and post-surface-labelling methods

## 6.3 Chelating agent-based labelling

The chelating agent-based radioisotope labelling method involves the use of a bifunctional chelating agent (BFC), such as 1,4,8,11-tetraazacyclotetradecane-1,4,8,11-tetraacetic acid (TATE), 4,11-bis(carboxymethyl)-1,4,8,11-tetraazabicyclo[6.6.2]hexadecane (CB-TE2A), (1,4,7-triazacyclononane-1,4,7-triacetic acid (NOTA), 1,4,7,10-tetraazacyclododecane-1,4,7,10-tetraacetic acid (DOTA) or desferrioxamine (DFO), which coordinate the metallic radioisotope including  $^{64}\text{Cu}$ ,  $^{177}\text{Lu}$ ,  $^{68}\text{Ga}$  and  $^{89}\text{Zr}$ , respectively<sup>[14-17]</sup> (Figure 3). The BFC method for radiolabelling has several advantages over other labelling methods. One advantage is that it provides stable and high-affinity binding of the radioisotope to the nanomaterial surface. BFCs have a high affinity for radioisotopes and can form stable complexes, which minimizes the risk of detachment of the radioisotope from the nanomaterial surface. This method also enables high specific activity labelling, which means that a high number of radioisotopes can be attached to a small amount of nanomaterial, resulting in improved sensitivity and accuracy in biodistribution studies. Overall, the BFC method provides a reliable and versatile approach for radiolabelling of nanomaterials for a variety of biomedical applications<sup>[18]</sup>.

The BFC terminal carboxyl, aldehyde, amino, thiol, silanol, or isothiocyanate groups are commonly covalently attached to the surface of nanoparticles (NPs) based on the coating layer applied during NP synthesis.<sup>[19-21]</sup> Although the chelating agent-based radioisotope labelling method has been widely used, the chemical modification of NPs through BFC incorporation can have potential drawbacks. This is because the addition of BFCs to NPs can alter their physical properties, such as size, surface charge and hydrophilicity, which can subsequently affect the overall biodistribution and pharmacokinetic behaviour of the labelled NPs.<sup>[22]</sup>



**Figure 3 — Structures of most popular BFCs employed for complexation with metallic radioisotopes**

In addition, selecting a suitable BFC to achieve optimal radioisotope labelling efficiency and stability poses a significant challenge due to the potential release of metallic radioisotope from the BFC and transchelation with endogenous proteins in vivo, resulting in suboptimal targeting that does not accurately represent the true biodistribution of radioisotope-labelled NPs.<sup>[23],[25]</sup> Additionally, the coordination chemistry of different metallic radioisotopes varies significantly, so a chelating agent can work well with one metallic radioisotope but not with others. Furthermore, certain metallic radioisotopes, such as <sup>72</sup>As, <sup>69</sup>Ge, and <sup>45</sup>Ti, still lack suitable chelating agents and radioisotope labelling methodologies. Therefore, new methods for radiolabelling NPs are highly desirable for the advancement of radioisotope-labelled nanomaterials.

## 6.4 Chelating agent-free radioisotope labelling method

### 6.4.1 General

To better understand the intrinsic behaviour of NPs and to avoid the influence of BFC, chelating agent-free labelling techniques have been developed. These methods eliminate the use of chelating agents and offer a relatively simple, versatile and promising approach for radioisotope labelling of NPs using a variety of metallic radioisotopes.<sup>[26]</sup> The nonclassical chelating agent-free radioisotope labelling methods are mainly divided into three categories and are discussed in detail by Goel et al. in a review.<sup>[27]</sup>

### 6.4.2 Radioactive-plus-non-radioactive precursors

The nonclassical method for synthesizing radioactive NPs is also known as the radiochemical doping method. This approach is relatively straightforward and involves adding a trace amount of a radioactive precursor to the core of a non-radioactive precursor. The small amount of radioactive precursor incorporates into the crystal lattice of the NPs, resulting in radioactive NPs that exhibit high stability and yield.

A wide variety of metallic radioisotopes can be used to synthesize radioisotope-labelled NPs. One example of this type is  $^{64}\text{Cu}$  radioisotope-labelled NPs reported by Zhou et al.,<sup>[28]</sup> which were synthesized by reacting radioactive  $^{64}\text{CuCl}_2$ , non-radioactive  $\text{CuCl}_2$ , and  $\text{Na}_2\text{S}$  in the presence of sodium citrate at 95 °C for 1 h. The average hydrodynamic particle size of the nanoparticle was 11 nm. The  $^{64}\text{Cu}$  NPs showed high stability in various media in vitro with no agglomeration and no change in hydrodynamic particle size for up to 7 d. Eventually, PEGylated  $^{64}\text{Cu}$  NPs showed high uptake in U87 human glioblastoma xenografts as a result of enhanced permeability and retention effects, which subsequently increased the synergetic effect of photothermal ablation therapy and radiotherapy at the target site.

Alvarez-Paneque et al.<sup>[29]</sup> synthesized Cu nanoparticles using gold (Au) as a template with controlled size and morphology. They prepared gold nanospheres with an average size of  $57,0 \pm 7,6$  nm and gold nanorods with a length of  $65,7 \pm 8,5$  nm and thickness of  $13,7 \pm 2,3$  nm, which were then coated with thiolated polyethylene glycol (mPEG-SH). Cu was introduced to the Au crystal lattice after reduction with hydrazine in the presence of poly(acrylic acid) as a stabilizer. Similarly, Sun et al.<sup>[30]</sup> doped  $^{64}\text{Cu}$  on Au-NPs of different sizes (10 nm, 30 nm and 80 nm) and shapes (sphere, rod and hexapod) using a similar methodology, which was found to be radiochemically stable in vivo. PET images were performed after injecting  $^{64}\text{Cu}$  Cu-Au (80 nm) NPs and  $^{64}\text{Cu}$  Cu-DOTA-Au (80 nm) NPs for comparison into mice via tail vein. At 1 h post-injection, a negligible amount of activity was observed in the bladder of mice injected with  $^{64}\text{Cu}$  Cu-Au (80 nm) NPs, while a significant amount of activity was observed in the bladder of mice injected with  $^{64}\text{Cu}$  Cu-DOTA-Au (80 nm) NPs, suggesting that the chelating agent released  $^{64}\text{Cu}$ , which was excreted from the kidney. This highlights the reliability and efficiency of the nonclassical and chelating agent-free method of radioisotope labelling compared to chelating agent-based methods. This was further confirmed by injecting  $^{64}\text{Cu}$  Cu-Au NR808 and co-injecting RGD- $^{64}\text{Cu}$  Cu-Au NR808 with a blocking agent.

Another example of the hot and cold precursor method is the synthesis of  $^{64}\text{Cu}$  CuAuNPs by allowing  $^{64}\text{Cu}$  to directly enter the lattice of AuNPs, as reported by Zhou et al.<sup>[31]</sup> In another study, glutathione-coated near-infrared (NIR) emitting radioactive gold NPs (GS- $^{198}\text{Au}$  AuNPs) were synthesized by adding  $\text{HAuCl}_4$  and  $\text{H}^{198}\text{AuCl}_4$  to a glutathione aqueous solution at 90 °C.<sup>[32]</sup>

### 6.4.3 Specific trapping

Specific trapping involves the absorption, entrapment, or reaction of radioisotopes into specific sites of NPs. This approach allows for fast and efficient direct radioisotope labelling of NPs without altering their behaviour in vivo and yields highly stable radioisotope-labelled NPs. Lin et al.<sup>[33]</sup> made an effort to load RGD<sub>4</sub>C, Cy5.5, and  $^{64}\text{Cu}$  simultaneously onto heavy-chain ferritins to produce nanoprobes for multimodal imaging targeting integrin  $\alpha_v\beta_3$ . Cy5.5 was chemically incorporated onto the ferritin surface, whereas RGD<sub>4</sub>D was introduced by amine coupling. Finally, bivalent  $^{64}\text{Cu}$  was loaded under acidic conditions by exploiting the nanocage-like structure of ferritin. The ferritin cavity is capable of binding to bivalent  $^{64}\text{Cu}$  with 60 % loading capacity, and free  $^{64}\text{Cu}$  was removed by a PD-10 column. It is believed that the hydrophilic channels in ferritin, which connect the inside and outside of ferritins, serve as a path to allow ions to enter the cavity. Once the ions enter the cavity of ferritin, they would find it hard to escape from it. It was found that only 10 % of the activity was released over a period of 24 h after incubation in phosphate-buffered



saline and fetal bovine serum. In vivo PET images were acquired by injecting hybrid probes into U87MG glioma tumour-bearing mice. The quantitative analysis showed continuous accumulation of activity in the tumour up to 24 h post-injection ( $6,4 \pm 1,7$  % ID/g after 1 h,  $7,5 \pm 0,7$  % ID/g after 4 h,  $8,1 \pm 0,1$  % ID/g after 24 h), which decreased to  $7,5 \pm 0,1$  % ID/g at 40 h post-injection. The EPR (enhanced permeability and retention) effect and active targeting were responsible for specific uptake in the tumour. The accumulation in the tumour mediated by the receptor was confirmed by performing blocking experiments, which showed that the uptake was significantly reduced.

Liu et al. [34] reported on the successful radioisotope labelling of  $^{64}\text{Cu}$  to  $\text{MoS}_2$ -IO-(d)PEG with a moderate radioisotope labelling yield of between 70 % to 85 % after 60 min of incubation at 37 °C. The  $^{64}\text{Cu}$  was absorbed onto the surface of  $\text{MoS}_2$  and remained intact for up to 48 h in serum. The feasibility of using [ $^{64}\text{Cu}$ ]Cu- $\text{MoS}_2$ -IO-(d)PEG NPs for PET imaging was established in 4T1 tumour-bearing mice at various time intervals. High accumulation and retention of [ $^{64}\text{Cu}$ ]Cu- $\text{MoS}_2$ -IO-(d)PEG was observed in the tumour of 4T1 tumour-bearing mice at 3 h post-injection, which was retained until 24 h.

A number of reports have demonstrated that fluorine-18 ( $^{18}\text{F}$ ) can be labelled to rare-earth NPs with high radiochemical yield and stability. Due to the short half-life of  $^{18}\text{F}$  ( $t_{1/2} = 110$  min), the radioisotope labelling procedures are necessarily simple, rapid, and efficient. In view of this, Li et al. synthesized tri-modal  $^{18}\text{F}$ -labelled  $\text{Na}_{0,20}\text{Bi}_{0,80}\text{O}_{0,35}\text{F}_{1,91} \cdot 20$  %Yb, 0,5 %Tm NPs ([ $^{18}\text{F}$ ]UNBOF) through a facile inorganic reaction between  $\text{Na}^{18}\text{F}$ ,  $\text{NH}_4\text{F}$ ,  $\text{NaNO}_3$ ,  $\text{Bi}(\text{NO}_3)_3$ , and  $\text{Ln}(\text{NO}_3)_3$  (Ln = Yb/Tm) under vigorous stirring within 1 minute at room temperature. Negligible dissociation of  $^{18}\text{F}$  was observed after incubating [ $^{18}\text{F}$ ]UNBOF NPs in fetal bovine serum, indicating strong interaction of  $^{18}\text{F}$  with NPs. [35]

Cui et al. synthesized trimodal  $\text{Fe}_3\text{O}_4@ \text{NaYF}_4$  core/shell inorganic nanoparticles for mapping lymph nodes (LNs). [36] Lanthanide elements Yb, Er, or Tm were doped into  $\text{NaYF}_4$  to achieve upconversion fluorescence, while Co was doped into  $\text{Fe}_2\text{O}_3$  to optimize the magnetic properties of  $(\text{Fe}_3\text{O}_4@ \text{NaYF}_4(\text{Yb}, \text{Tm}))$  and  $(\text{Co}_{0,16}\text{Fe}_3\text{O}_4@ \text{NaYF}_4(\text{Yb}, \text{Er}))$  NPs. The NPs' surfaces were modified by incorporating bisphosphonate polyethylene glycol (BP-PEG) to improve their surface properties and solubility. Subsequently,  $^{18}\text{F}$  was labelled onto the NPs with a radioisotope labelling yield of up to 38 % in just 5 min at room temperature. The resulting  $^{18}\text{F}$ -labelled  $\text{Co}_{0,16}\text{Fe}_3\text{O}_4@ \text{NaYF}_4(\text{Yb}, \text{Er})$ -BP-PEG and  $\text{Fe}_3\text{O}_4@ \text{NaYF}_4(\text{Yb}, \text{Tm})$ -BP-PEG NPs were found to be stable in human serum for up to 2 h, with 85 % of the activity remaining attached to the NPs. The NPs' in vivo PET/MRI imaging capabilities were evaluated for the detection of popliteal LNs in response to an acute inflammatory stimulus in the foot. A solution of  $^{18}\text{F}$ -labelled NPs was injected into the mouse's footpad, and both popliteal and iliac LNs were visible in PET and MRI images 6 h post-injection.

#### 6.4.4 Cation exchange

The cation exchange method is an alternative doping technique used for the synthesis of nanocrystals, whereby the pre-existing cation in the nanomaterials is substituted with a different cation. This method is promising as it allows for the production of NPs that cannot be synthesized directly, due to the fast reaction kinetics at room temperature.

Recently, Tang et al. [37] synthesized zinc sulfide ( $\text{ZnS}$ ) quantum dot nanocrystals (QDs) using 3-mercaptopropionic acid as a capping agent. Thiol-functionalized polyethylene glycol ( $\text{SH-PEG-OCH}_3$ ) was incorporated onto the surface of the QDs ( $\text{QD-OCH}_3$ ) to improve their stability and biocompatibility. The  $\text{QD-OCH}_3$  was rapidly labelled with  $^{68}\text{Ga}$  or  $^{64}\text{Cu}$  within 15 min at 37 °C in a sodium acetate buffer with radiochemical efficiency > 95 % for  $^{68}\text{Ga}$  and > 90 % for  $^{64}\text{Cu}$ . The  $^{64}\text{Cu}$ -labelled  $\text{QD-OCH}_3$  showed high stability in a 1,8 mM DOTA and DTPA chelating agent solution in PBS, with most of the activity remaining attached to  $\text{QD-OCH}_3$ . The stability against other metal ions, such as ferric chloride (1,8 mM), was also tested, and the results showed that only a small portion (approximately 1,9 %) of radioactivity was released from the  $^{68}\text{Ga}$ -labelled  $\text{QD-OCH}_3$ . In vivo PET imaging of [ $^{64}\text{Cu}$ ]Cu- $\text{QD-OCH}_3$  in 4T1 mouse breast tumour xenograft clearly showed tumour tissue at 3 h and 24 h post-injection scan. In contrast, the control group [ $^{64}\text{Cu}$ ]Cu-DOTA showed only bladder uptake at 3 h post-injection, indicating rapid renal clearance.

Sun et al. [38] developed a self-illuminating QD system by directly doping trace amounts of  $^{64}\text{Cu}$  into  $\text{CdSe}/\text{ZnS}$  core/shell QDs via a cation-exchange reaction for luminescence and PET imaging. The  $^{64}\text{Cu}$  radioisotope was labelled via cation exchange with 100 % radiochemical efficiency and showed high stability in fetal bovine serum and mouse blood at 37 °C for 48 h. The  $^{64}\text{Cu}$ -labelled QDs were modified with amine-polyethylene glycol-thiol (amine-PEG5000-thiol) to increase water solubility. The in vivo distribution of  $^{64}\text{Cu}$ -doped QDs was studied in a U87MG glioblastoma xenograft model using PET. Mice were injected with

25 µg QD580 (250 µCi of  $^{64}\text{Cu}$ ) via the tail vein, and PET scans were obtained at 1 h, 17 h, 24 h and 42 h post-injection. Quantitative analysis (ROI) of the whole-body PET image showed 5 % ID/g uptake in the U87MG glioblastoma tumour site, which further increased to 12 % ID/g at 17 h post-injection, and after 42 h, 10 % ID/g of the QDs was still retained in the tumour.

#### 6.4.5 Neutron or proton beam activation

This strategy involves the synthesis of nonradioactive NPs, which are then converted into radioactive NPs through direct irradiation by a proton beam or thermal neutron.

Wang et al.[39] synthesized carbon nanocapsules filled with nonradioactive Samarium-152 ( $^{152}\text{Sm}$ ) isotopes ( $^{152}\text{Sm@SWNT}$  and  $^{152}\text{Sm@MWNT}$ ) and then activated them through neutron irradiation to create  $^{153}\text{Sm}$  for therapeutic use. The loading capacity of  $^{152}\text{Sm}$  was determined to be approximately 12,3 % mass fraction for  $^{152}\text{Sm@SWNT}$  and 17,6 % mass fraction for  $^{152}\text{Sm@MWNT}$ , using inductively coupled plasma mass spectrometry (ICP-MS). After irradiation in high neutron flux ( $1,6 \times 10^{14} \text{ n cm}^{-2}\text{s}^{-1}$ ) and long neutron irradiation time, high specific activities of [ $^{153}\text{Sm}$ ]Sm@SWNT (6,33 GBq/mg) and [ $^{153}\text{Sm}$ ]Sm@MWNT (11,37 GBq/mg) were obtained. SPECT/CT imaging showed that both [ $^{153}\text{Sm}$ ]Sm@SWNTs and [ $^{153}\text{Sm}$ ]Sm@MWNT had similar biodistribution patterns, with activity mostly accumulating in spleen, lung and liver at 30 min post-injection and retaining up to 24 h post-injection. Quantitative  $\gamma$ -counting measurement validated the distribution pattern of radioactivity. Additionally, the study demonstrated that the conjugates [ $^{153}\text{Sm}$ ]Sm@SWNTs and [ $^{153}\text{Sm}$ ]Sm@MWNT were therapeutically effective in delaying the growth of metastatic lung tumours..

Holmium-166 ( $^{166}\text{Ho}$ ) is a promising therapeutic radionuclide that emits high-energy  $\beta$  particles ( $E_{\text{max}} = 1,84 \text{ MeV}$ ) and has a long half-life of 26,8 h. One way to prepare  $^{166}\text{Ho}$ -labelled nanoparticles (NPs) is by neutron activation of the stable isotope  $^{165}\text{Ho}$ , which produces high specific activity. Di Pasqua et al.[40] have successfully prepared  $^{165}\text{Ho}$ -doped mesoporous silica type MCM-14 ( $^{165}\text{Ho-MSNs}$ ) NPs with a particle size of 80 nm – 100 nm in diameter. Subsequently,  $^{165}\text{Ho-MSNs}$  were irradiated in a reactor (1 MW) at a thermal neutron flux of approximately  $5,5 \times 10^{12} \text{ neutrons/cm}^2\text{s}$  for 1 h to 18 h to produce [ $^{166}\text{Ho}$ ]Ho-MSNs. In a study, the biodistribution of [ $^{166}\text{Ho}$ ]Ho-MSNs was evaluated after intraperitoneal injection in SKOV-3 ovarian tumour-bearing xenografts. The results showed high accumulation of the NPs in the tumour (32,8 % ID/g  $\pm$  68,1 % ID/g) at 24 h post-injection, which increased to approximately 2,5 times (81 % ID/g  $\pm$  7,5 % ID/g) at 1 week post-injection. This indicates that [ $^{166}\text{Ho}$ ]Ho-MSNs have the potential to be used as an effective therapeutic agent for the treatment of ovarian tumours.

Proton beam activation of metal oxide NPs via (p,n), (p, $\alpha$ ) nuclear reactions has been reported by Pérez Campaña et al.[41-43] In one study, Pérez Campaña et al.[41] prepared  $^{18}\text{O}$ -enriched aluminium oxide ( $\text{Al}_2\text{O}_3$ ) NPs in the presence of basic aqueous media, followed by activation via the  $^{18}\text{O}(\text{p},\text{n})^{18}\text{F}$  nuclear reaction with a 16 MeV proton. The irradiation with 16 MeV did not significantly change the particle size of the  $\text{Al}_2\text{O}_3$  NPs, confirming their high stability before and after irradiation.

In a follow up study Pérez-Campaña et al.[43] prepared  $^{18}\text{O}$ -enriched titanium dioxide ( $\text{TiO}_2$ ) NPs by bubbling  $\text{NH}_3(\text{g})$  through an aqueous solution of  $\text{TiCl}_4$  in the presence of  $^{18}\text{O}$ -enriched water ( $[^{18}\text{O}]\text{H}_2\text{O}$ ) as a solvent under an inert atmosphere to avoid incorporation of  $^{16}\text{O}$  and  $\text{NH}_3$ . The resulting  $\text{TiO}_2$  NPs were irradiated with a 15 MeV proton for 6 min at a beam intensity of 5 µA. This converted the  $^{18}\text{O}$ -enriched  $\text{TiO}_2$  NPs to  $^{18}\text{F}$ -labelled NPs via the  $^{18}\text{O}(\text{p},\alpha)^{18}\text{F}$  nuclear reaction, producing high amounts of  $^{18}\text{F}$  ( $\approx 700 \text{ kBq mg}^{-1}$ ) in a short irradiation time. This amount of radioactivity produced is sufficient for in vivo assessment and distribution monitoring of NPs by PET/CT imaging. The  $^{18}\text{F}$ -labelled  $\text{TiO}_2$  NPs were administered intravenously, and PET/CT images were obtained at different time intervals.

### 6.5 Dual radioisotope labelling

Dual radioisotope labelling is a technique that allows the fate of different components of a nanoparticle, such as the inorganic core, the organic surface capping and the protein corona, to be traced individually. Typically, this is achieved by labelling both the core and surface with different radioisotopes. This technique enables the integrity of radioisotope labelling on the surface of nanomaterials to be evaluated.

Here is a typical example of dual isotope labelling using gold nanoparticle.[44] The authors used  $^{197}\text{Au}$ , a stable isotope, to create the gold nanoparticle, which was then stabilized by a ligand shell of dodecanethiol. Following neutron activation, some of the Au atoms were converted into the radioactive isotope  $^{198}\text{Au}$ ,



to form the radioisotope-labelled core. To make the nanoparticle water-soluble, a shell of the amphiphilic polymer poly(isobutylene-alt-maleic anhydride)-graft-dodecyl was wrapped around the Au core. DOTA was integrated into the polymer shell and loaded with indium (enriched with the radioisotope  $^{111}\text{In}$ ), which acted as the shell label. In this way, the nanoparticle core and shell were individually labelled by  $^{198}\text{Au}$  and  $^{111}\text{In}$ , respectively. After administering [ $^{111}\text{In}$ ]In-DTPA-[ $^{198}\text{Au}$ ]gold nanoparticle into normal mice, the authors traced the radioactivity using tissue-based biodistribution techniques. They found that the polymer shells of polymer-coated Au nanoparticles were partially removed both in vitro and in vivo. In vivo, the nanoparticles were mostly retained in the liver, and fragments of the organic shell were excreted through the kidneys. The authors suggested that proteolytic enzymes present in these compartments caused a partial separation of the organic shell from the inorganic core. They also noted that the amide bond linkage for connection of a shell and BFC can cause the bond breakage by the enzyme. In contrast, using a different linkage, such as thiourea, resulted in in vivo integrity after administration<sup>[45]</sup>.

## 6.6 Choice of radioisotopes

The abundance of radioisotopes varies widely in terms of half-life and chemical properties, ranging from alkali metals to lanthanides. Due to this diversity, it is important to select the appropriate radioisotope for labelling nanomaterials for in vivo animal experiments. Characteristics such as decay half-life, decay energy and availability of the isotope are also considered when choosing the ideal radioisotope for labelling (see [Annex A](#)). Commonly used radioisotopes include generator-produced  $^{68}\text{Ga}$ ,  $^{99\text{m}}\text{Tc}$  or  $^{188}\text{Re}$ ; cyclotron-produced  $^{18}\text{F}$ ,  $^{64}\text{Cu}$ ,  $^{89}\text{Zr}$ ,  $^{111}\text{In}$ ,  $^{123}\text{I}$  or  $^{124}\text{I}$ ; and reactor-produced  $^{125}\text{I}$  or  $^{177}\text{Lu}$ . For in vivo biodistribution studies, radioisotopes that emit  $\gamma$ -rays are typically used. Positron-emitting radioisotopes also emit  $\gamma$ -rays after the annihilation reaction. The physical half-life of radioisotopes is also a significant consideration. Radioisotopes with short half-lives, such as  $^{18}\text{F}$  ( $t_{1/2} = 109,8$  min),  $^{68}\text{Ga}$  ( $t_{1/2} = 67,7$  min) and  $^{99\text{m}}\text{Tc}$  ( $t_{1/2} = 6$  h), or those with longer half-lives, such as  $^{64}\text{Cu}$  ( $t_{1/2} = 12,7$  h),  $^{111}\text{In}$  ( $t_{1/2} = 67$  h), and  $^{89}\text{Zr}$  ( $t_{1/2} = 78,4$  h), are chosen based on the biodistribution study's purpose. The physical half-life of a radioisotope can be matched with the biological half-life of the nanomaterials being labelled with these radioisotopes to allow them to reach the targets of interest. It is also crucial to keep the decay time as short as possible to minimize radiation exposure. Long-lived isotopes, such as  $^{89}\text{Zr}$ , are preferred for monitoring clearance profiles of nanomaterials.<sup>[46,47]</sup> To select the appropriate radioisotope for labelling of nanomaterials, several factors can be considered, including (1) desirable decay characteristics of the radionuclide to produce high-quality images, (2) the availability of methods to produce the radioisotope in sufficient and pure quantities, (3) efficient radioisotope labelling methodologies and most importantly, (4) the physical half-life of the radionuclide. It is crucial that the half-life is long enough to allow sufficient time for monitoring pharmacokinetics (target tissue uptake and elimination) and biodistribution, as well as for the transportation of the radioisotope-labelled material to the preclinical or clinical site.<sup>[48]</sup>

## 6.7 Production of radioisotopes

### 6.7.1 General

In clinical settings, radioisotopes are predominantly artificial and typically produced in particle accelerators, cyclotrons, or reactors. The specific radionuclide produced depends on factors such as the type of irradiating particle, its energy and the target nuclei. However, the high cost and limited availability of these facilities means that remote facilities without such equipment rely on the supply of radionuclides from external sources. Short-lived radionuclides, in particular, decay rapidly and are only available at institutions with cyclotron or reactor facilities, making it difficult to supply them to remote hospitals or institutions. To address this issue, radionuclide generators provide a secondary source of radionuclides, particularly short-lived ones.<sup>[49]</sup>

The purification of crude radioactive products to obtain a pure radioisotope with high specific activity is crucial. In a specific irradiating system, different isotopes of various elements can be produced, requiring the isolation of isotopes of a single element. This can be achieved by utilizing suitable chemical methods such as solvent extraction, precipitation, ion exchange and distillation. It is crucial to consider the chemical characteristics of each radioisotope when selecting the appropriate purification method.<sup>[50]</sup>

### 6.7.2 Cyclotron-produced radioisotopes

A medical cyclotron is a circular particle accelerator that was originally proposed by Ernest O. Lawrence in 1929. It is essentially a modified version of a linear accelerator, designed to be smaller in size. Cyclotrons operate by accelerating charged particles, such as protons, deuterons, hydrides,  $\alpha$  particles and  $^3\text{He}$  particles, in circular paths within dees under a high electromagnetic field, while maintaining a vacuum. As the charged particles move in circular paths under the magnetic field, their energy gradually increases. The larger the radius of the particle trajectory, the higher the energy of the particle. The energy of the particles produced by the cyclotron can range from a few keV to several hundred MeV, depending on the design and type of the cyclotron. Medical cyclotrons generally have an accelerating capacity of less than 30 MeV for particles. Cyclotron-produced radioisotopes are typically neutron deficient and decay via  $\beta^+$  emission or electron capture, resulting in a relatively higher specific activity compared to reactor-produced radioisotopes. [Table 1](#) lists several examples of cyclotron-produced radioisotopes that emit  $\gamma$  or  $\beta^+$  radiation.<sup>[51]</sup>

Several radioisotopes are commonly used in medical imaging.  $^{67}\text{Ga}$ ,  $^{123}\text{I}$ ,  $^{111}\text{In}$  and  $^{201}\text{Tl}$  are used for gamma camera or SPECT imaging, while  $^{11}\text{C}$ ,  $^{13}\text{N}$ ,  $^{15}\text{O}$ ,  $^{18}\text{F}$ ,  $^{64}\text{Cu}$  and  $^{124}\text{I}$  are used for PET imaging. Radioisotopes with longer half-lives, such as  $^{18}\text{F}$ ,  $^{64}\text{Cu}$ ,  $^{67}\text{Ga}$ ,  $^{123}\text{I}$ ,  $^{124}\text{I}$ ,  $^{111}\text{In}$  and  $^{201}\text{Tl}$ , can be purchased from companies, if available, as they can be transported to different sites before decay. However, radioisotopes with half-lives less than 20 min, such as  $^{11}\text{C}$ ,  $^{13}\text{N}$  and  $^{15}\text{O}$ , can be produced on site due to their short half-lives.

**Table 1 — Commonly used cyclotron-produced radioisotopes**

Radioisotopes	Physical half-life	Decay mode (%)	$\gamma$ -Ray energy (MeV)	Abundance (%)
$^{11}\text{C}$	20,4 min	$\beta^+$ (100)	0,511	200
$^{13}\text{N}$	9,96 min	$\beta^+$ (100)	0,511	200
$^{15}\text{O}$	2,03 min	$\beta^+$ (100)	0,511	200
$^{18}\text{F}$	109,8 min	$\beta^+$ (97), EC <sup>a</sup> (3)	0,511	194
$^{64}\text{Cu}$	12,8 h	$\beta^+$ (19) or $\beta^-$ (40), EC (41)	0,511	38,6
$^{67}\text{Ga}$	3,3 d	EC (100)	0,093, 0,184, 0,300	40, 20, 17
$^{111}\text{In}$	2,8 d	EC (100)	0,171, 0,245	90, 94
$^{123}\text{I}$	13,2 h	EC (100)	0,159	83
$^{124}\text{I}$	4,2 d	$\beta^+$ (23), EC (77)	0,511	46
$^{201}\text{Tl}$	73 h	EC (100)	0,167	9,4 (X-ray: 93)

<sup>a</sup> EC: electron capture.

### 6.7.3 Reactor-produced radioisotopes

Radioisotopes can be produced in large quantities in nuclear reactors. However, their relatively low specific activity limits their use, except for radioisotopes like  $^{131}\text{I}$  or certain mother radionuclides used in generators, which have established purification methods. In recent years, the use of therapeutic radioisotopes such as  $^{177}\text{Lu}$ ,  $^{225}\text{Ac}$  and  $^{212}\text{Pb}$  has dramatically increased, leading to an expansion of the industry for reactor-produced radioisotopes.

A nuclear reactor operates using fuel rods made of fissile materials, such as enriched  $^{235}\text{U}$  and  $^{239}\text{Pu}$ . These fuel nuclei undergo spontaneous fission, which is the breakup of a heavy nucleus into two fragments of approximately equal mass, accompanied by the emission of two to three neutrons with mean energies of about 1,5 MeV. If the right conditions exist, neutrons emitted in one fission reaction can cause further fission of other fissionable nuclei in the fuel rod, initiating a nuclear chain reaction. To control this chain reaction, the fuel materials are designed to limit the number of free neutrons available for further fission. The high-energy neutrons produced in the fission process, known as fast neutrons, are slowed down to create thermal neutrons through interaction with a moderator, such as water, heavy water or graphite. The moderator is distributed in the spaces between the fuel rods and helps to maintain a stable chain reaction. Two types of interaction with thermal neutrons are significant for the production of various useful radionuclides: fission (n, f) reaction of heavy elements and neutron capture (n,  $\gamma$ ) reaction. Clinically useful radionuclides such as  $^{131}\text{I}$  and  $^{99}\text{Mo}$  are produced from the fission reaction of  $^{235}\text{U}$ . Many other nuclides are also produced from

the fission of  $^{235}\text{U}$ , and the crude fission products are purified using the appropriate method. The fission products are typically neutron-rich and decay by  $\beta^-$  emission. In the neutron capture reaction, the target nucleus captures one thermal neutron and emits  $\gamma$ -rays to produce an isotope of the same element. The radionuclide produced by the neutron capture reaction has relatively low specific activity, making this method impractical for producing clinically useful radionuclides. Therefore, neutron capture reaction is primarily used for trace metal analysis with neutron activation analysis. The (n, p) or (n,  $\alpha$ ) reaction in the reactor is also useful for the production of  $^{14}\text{C}$ ,  $^{32}\text{P}$  or  $^3\text{H}$ .<sup>[52]</sup>

#### 6.7.4 Generator-produced radioisotopes

In 1926, Failla designed and used the first generator for clinical applications.<sup>[53]</sup> The use of radioisotope generators has become increasingly popular due to their convenience and cost-effectiveness compared to cyclotron- or reactor-produced radioisotopes. This has led to the development of various radioisotope generators that serve as convenient sources of radioisotope production. The structure of a radionuclide generator is relatively simple, consisting of a column and a shielded container. The column is filled with an adsorbent material such as cation- or anion-exchange resin, aluminium oxide, titanium oxide or tin oxide, on which the parent nuclide is adsorbed. The daughter radioisotope grows as a result of the decay of the parent until either a transient or a secular equilibrium is reached within several half-lives of the daughter. Since there are differences between the mother and the daughter radioisotope in chemical properties, the daughter activity is eluted in a carrier-free state with an appropriate solvent, leaving the parent on the column. After one elution, the daughter activity starts to grow again in the column until an equilibrium is reached in which the daughter appears to decay with the same half-life as the parent. Therefore, the elution of activity can be made repeatedly.

An ideal radioisotope generator for nuclear medicine can be sterile, pyrogen-free and easy to use, providing a high yield of daughter radioisotope repeatedly and reproducibly. Numerous radioisotope generator systems have been developed, but only a few are commonly used in routine nuclear medicine practice. These important generators include the  $^{99}\text{Mo}$ - $^{99\text{m}}\text{Tc}$ ,  $^{68}\text{Ge}$ - $^{68}\text{Ga}$ ,  $^{82}\text{Sr}$ - $^{82}\text{Rb}$  and  $^{188}\text{W}$ - $^{188}\text{Re}$  systems, which are listed in Table 2 along with their properties. The  $^{99}\text{Mo}$ - $^{99\text{m}}\text{Tc}$  generator is the most widely used generator system in nuclear medicine due to the excellent radiation characteristics of  $^{99\text{m}}\text{Tc}$ . This system offers a 6 h half-life, minimal electron emission, and a high yield of 140 keV  $\gamma$ -rays (90 %), making it ideal for imaging devices in nuclear medicine. The  $^{68}\text{Ge}$ - $^{68}\text{Ga}$  and  $^{82}\text{Sr}$ - $^{82}\text{Rb}$  generator systems are utilized for PET radiopharmaceuticals, while the  $^{188}\text{W}$ - $^{188}\text{Re}$  generator is used for the therapeutic application of  $^{188}\text{Re}$ -labelled radiopharmaceuticals.

**Table 2 — Commonly used radioisotope generator systems**

System	Parent half-life	Daughter half-life	Decay mode	$\gamma$ -Energy (keV)	Eluent
$^{99}\text{Mo}$ - $^{99\text{m}}\text{Tc}$	66 h	6 h	IT <sup>a</sup>	140	0,9 % NaCl
$^{68}\text{Ge}$ - $^{68}\text{Ga}$	271 d	68 min	$\beta^+$	511	0,1 M HCl
$^{82}\text{Sr}$ - $^{82}\text{Rb}$	25,5 d	75 sec	$\beta^+$	511	0,9 % NaCl
$^{188}\text{W}$ - $^{188}\text{Re}$	69,4 d	17 h	$\beta^-(2,1 \text{ MeV})$ , $\gamma$	155	0,9 % NaCl

<sup>a</sup> IT: isomeric transition.

#### 6.8 Chelating agent and the matched pair for radioisotope

Almost all metallic radioisotopes require a chelating agent or bifunctional chelating agent (BCA) to connect with nanomaterials. However, the metallic radioisotopes of choice are diverse in their coordination chemistry, making it challenging to find a suitable chelating agent or BCA that works with all radioisotopes. Several factors can be considered when selecting a chelating agent or BCA for a specific radioisotope, such as the coordination number of the metal ion, the matching cavity size of the chelating agent or BCA with the ionic radius of the ion, the oxidation state of the metal ion, the hardness or softness of the ion, providing the appropriate chelate density or number of donor binding groups, and the rate of complex formation and dissociation.<sup>[54]</sup> Therefore, the ideal goal for selecting a chelating agent or BCA for a specific radioisotope is to achieve instant radioisotope complex formation with infinite in vitro or in vivo stability or no dissociation.

There are various types of chelating agents or BCA that have been reported to be labelled with radioisotopes, including both acyclic and macrocyclic compounds (as shown in [Figure 3](#)). Initially, bifunctional ethylenediaminetetraacetic acid (EDTA) derivatives were used for labelling with  $^{111}\text{In}$  and  $^{90}\text{Y}$ , but their stability issues led to the development of bifunctional diethylenetriaminepentaacetic acid (DTPA) derivatives, which offer a more appropriate coordination number and improved complex stability.<sup>[55],[56]</sup>

To enhance the overall stability of the radionuclide-chelator complex and minimize potential toxicity, researchers have developed a variety of modified chelators. One example is Cy-DTPA, in which one ethylene group of DTPA is modified with a cyclohexyl carbon chain. This modified chelator has been used to label several radionuclides, including  $^{90}\text{Y}$ ,  $^{111}\text{In}$ ,  $^{177}\text{Lu}$  and  $^{213}\text{Bi}$ , resulting in stable complexes.<sup>[57]</sup> However, even with these modifications, the overall stability of radionuclide-chelator complexes can still be less than ideal and can contribute to toxicity concerns.<sup>[58]</sup>

Hexadentate macrocyclic bifunctional 1,4,7-triazacyclononane-1,4,7-triacetic acid (NOTA) derivatives have been reported for labelling with  $^{111}\text{In}$ .<sup>[59]</sup> Although NOTA derivatives are well known to form highly stable complexes with  $^{68}\text{Ga}$ , for radio-lanthanide labelling, DOTA derivatives are a better choice than NOTA derivatives.<sup>[60]</sup>

Octadentate macrocyclic bifunctional 1,4,7,10-tetraazacyclododecane-1,4,7,10-tetraacetic acid (DOTA) derivatives have been developed for  $^{90}\text{Y}$ ,  $^{111}\text{In}$  and radio-lanthanides, and these complexes have shown better stability than acyclic BCA complexes.<sup>[61-64]</sup> Although a large number of the DOTA application for radionuclide therapy have been reported, the limitation to use of the DOTA derivatives still remains; slower complex formation rate and thereof the heating process is needed for radioisotope labelling.<sup>[65,66]</sup>

There are larger-sized chelating agents, such as 1,4,7,10,13-pentaazacyclododecane-1,4,7,10,13-pentaacetic acid (PEPA) or 1,4,7,10,13,16-hexaazacyclododecane-1,4,7,10,13,16-hexaacetic acid (HEHA), which are designed for larger ionic radii of radioisotopes. However, PEPA and HEHA have been found to exhibit decreased kinetic inertness and thermodynamic stability due to their higher flexibility in the chelating agent framework.<sup>[67]</sup>

A macrocyclic BCA with a 14-membered ring, 1,4,8,11-tetraazacyclotetradecane-1,4,8,11-tetraacetic acid (TETA) derivative, has been reported for labelling with  $\text{Cu(II)}$  only, and is not suitable for other radionuclides.<sup>[68,69]</sup>

For the treatment of bone metastasis using radionuclide therapy, several chelating agents containing phosphorous have been developed, including hydroxyethylidinediphosphonic acid (HEDP), ethylenediamine-N,N,N',N'-tetrakis(methylenephosphonic acid) (EDTMP), and 1,4,7,10-tetraazacyclododecane-1,4,7,10-tetraaminomethylenephosphonic acid (DOTMP). HEDP has been utilized for complex formation with  $^{186}\text{Re}$  or  $^{188}\text{Re}$ ,<sup>[70,71]</sup> while EDTMP or DOTMP have been used for  $^{177}\text{Lu}$  or  $^{212}\text{Bi}$ .<sup>[72,73]</sup>

Diaminedithiol ( $\text{N}_2\text{S}_2$ ) derivatives have been utilized for the formation of complexes with  $^{99\text{m}}\text{Tc}$  and  $^{188}\text{Re}$ , and have been reported for their use in the diagnosis or treatment of liver cancer.<sup>[74-76]</sup>

BCAs used for conjugation to nanomaterials typically consist of two chemical parts: a chelating part for the radioisotope and a covalent linkage part for attaching to the nanomaterial. The chelating part forms a complex with the radioisotope, while the linkage part enables the complex to be attached to the nanomaterial. Common examples of linkage chemistry include conjugation of an active ester, isothiocyanate, or maleimide group on the BCA to an amino or thiol group on the nanomaterial. The choice of conjugation method depends on the chemical compatibility of the BCA and nanomaterial, and the optimal method is selected based on the ease of modification.

## 7 The stability of radioisotope-labelled nanomaterials

There are several factors that affect the stability of radioisotope-labelled nanomaterials, including the radioisotope-labelled part (e.g. chelating agent, linker) and the nanomaterial itself. Nanomaterials used for in vitro diagnostic or in vivo applications can be modified or coated with a biologically inert material to reduce unwanted interactions with blood, serum, urine, etc. This can improve stability, optimize in vivo pharmacokinetics, and incorporate diagnostic or disease-targeting moieties. Without proper surface coating, most nanomaterials, especially those with hydrophobic surfaces, tend to aggregate or agglomerate into large clusters in the test field of in vitro diagnostics or in vivo settings due to hydrophobic interactions or Van der Waals forces. Even for nanomaterials with good inherent aqueous dispersity, surface coating can



be beneficial for maintaining their structural integrity. Polyethylene glycol (PEG) is the most widely used synthetic polymer in the drug delivery field due to its long history of safety in humans. The length, shape, or charge of PEG can also affect the stability or biodistribution of nanomaterials.<sup>[77],[78]</sup>

Maintaining in vivo integrity of radioisotope-labelled nanomaterials is crucial for accurate measurement of their pharmacokinetics or toxicokinetics. Several factors can be considered, including the linker used to conjugate the nanomaterials and radioisotope-labelled chelating agent, as well as the chelating interaction between the chelating agent and radioisotope. Linkers can be hydrocarbon chains or peptide sequences, but if they contain an amide bond, they can be cleaved by amidases in plasma, resulting in the detachment of the radioisotope label from the nanomaterial. In some studies, the chelating agent-based radioisotope labelling has been reported to be detached from nanomaterials due to proteolytic digestion,<sup>[44]</sup> while in other studies, the labelling remained intact. Further research is needed to resolve these discrepancies and fully understand the fate of radioisotope-labelled nanomaterials. Nonetheless, it is essential to confirm the in vivo integrity of these materials to ensure accurate evaluation of their pharmacokinetics and toxicokinetics.<sup>[43],[79]</sup>

Another important factor for in vivo stability, which can significantly impact the biodistribution and pharmacokinetics of nanomaterials, is the thermodynamic stability of the complex formed between the radioisotope and the chelating agent. An example illustrating this is the phenomenon of transchelation in living animals involving superoxide dismutase (SOD) in the liver. Bass et al. conducted a study where they labelled a peptide with  $^{64}\text{Cu}$  and observed high liver uptake, indicating transchelation of  $^{64}\text{Cu}$  into SOD in the rat liver.<sup>[80]</sup> They used TETA as the chelating agent, which is commonly used for  $^{64}\text{Cu}$  labelling, but the thermodynamic stability of the copper-TETA complex is known to be low. Therefore, it is crucial to consider the possibility of in vivo transchelation resulting from the thermodynamic instability of the complex and carefully select the appropriate radioisotope-chelating agent pair based on the literature.<sup>[81]</sup>

## 8 Advantages and disadvantages of radioisotope labelling method

For the selection of a radioisotope labelling method for nanomaterials, various factors are carefully considered, including the specific purpose of the radioisotope labelling, the physicochemical properties of the nanomaterial, the in vitro or in vivo stability of the nanomaterial itself, and the desired time window for biodistribution studies. With these factors in mind, a suitable radioisotope and compatible chelating agent can be chosen. This document focuses on five different types of radioisotope labelling methods, each with its own advantages and disadvantages (see [Annex B](#)).

For the successful chelating agent-based radioisotope labelling of nanomaterials, various factors are carefully considered, including the selection of the appropriate chelating agent, optimization of radioisotope labelling conditions and the use of stable linkers suitable for the desired biodistribution study time frame.<sup>[82],[83]</sup> A thorough understanding of the labelling chemistry is essential for achieving successful results. Compared to other methods, chelating agent-based radioisotope labelling is relatively straightforward and generates fewer radioactive wastes during the purification step. However, it is important to consider the potential enzymatic cleavage of the linker by specific enzymes present in serum. On the other hand, alternative methods that do not involve chelating agents are gaining attention due to their potential for more stable and specific radioisotope labelling of nanomaterials. Nonetheless, these chelating agent-free methods can produce more radioactive waste during the purification process compared to chelating agent-based radioisotope labelling methods.<sup>[84]</sup>

## Annex A

### (informative)

## Representative radioisotopes used for nanomaterial labelling

**Table A.1 — Representative radioisotopes used for nanomaterial labelling**

Radioisotopes	Physical half-life	Decay mode (%)	$\gamma$ -Ray energy (MeV)
$^{18}\text{F}$	109,8 min	$\beta^+$	634
$^{68}\text{Ga}$	67,7 min	$\beta^+$	770, 1 890
$^{64}\text{Cu}$	12,7 h	$\beta^-$ , $\beta^+$	511, 653
$^{44}\text{Sc}$	3,9 h	$\beta^+$ (94), EC (6)	1,474 1,157
$^{89}\text{Zr}$	3,3 d	$\beta^+$ (23), EC (77)	897
$^{67}\text{Ga}$	3,3 d	EC (100)	0,093, 0,184, 0,300
$^{111}\text{In}$	2,8 d	EC (100)	0,171, 0,245
$^{99\text{m}}\text{Tc}$	6,0 h	$\gamma$	141
$^{124}\text{I}$	4,2 d	$\beta^+$ (23), EC (77)	0,511

## Annex B

### (informative)

## Advantages and disadvantages of radioisotope labelling methods for nanomaterials

**Table B.1 — Advantages and disadvantages of radioisotope labelling methods for nanomaterials**

	<b>Chelating agent-based</b>	<b>Radioactive + non-radioactive</b>	<b>Specific trapping</b>	<b>Cation exchange</b>	<b>Activation</b>
Advantages	Surface labelling Commonly used Easy labelling Less radioactive waste	Core-labelling Show real fate of NPs No linker	Core-surface labelling No linker	Core-surface labelling No linker	Core-labelling Show real fate of NPs No linker
Disadvantages	Bond breakage in the linker	More radioactive waste	Rare cases Transmetalation	Rare cases Transmetalation	Rare cases Less radioactivity Needs high-energy particles

## Bibliography

- [1] STRINGER R.E., *RADIOCHEMICAL METHODS / Pharmaceutical Applications*, in Encyclopedia of Analytical Science (Second Edition), WORSFOLD P., TOWNSHEND A., POOLE C., Editors. 2005, Elsevier: Oxford. p. 86-93.
- [2] FAQI A.S. A Comprehensive Guide to Toxicology in Nonclinical Drug Development ( Second Edition) FAQI A.S., Editor. 2017, Academic Press: Boston. p. 1-4.
- [3] SILVA LIMA B., VIDEIRA M.A., Toxicology and Biodistribution: The Clinical Value of Animal Biodistribution Studies. Molecular therapy. Methods & clinical development, 2018. **8**: p. 183-197.
- [4] DING H., WU F., Image guided biodistribution and pharmacokinetic studies of theranostics. Theranostics, 2012. **2**(11): p. 1040-53.
- [5] TURNER S.M., HELLERSTEIN M.K., Emerging applications of kinetic biomarkers in preclinical and clinical drug development. Curr Opin Drug Discov Devel, 2005. **8**(1): p. 115-26.
- [6] STUMPF W.E. *Autoradiography: advances in methods and application*. J Histochem Cytochem, 1981. **29**(1A Suppl): p. 107-8.
- [7] SKOTLAND T. et al., Biodistribution, pharmacokinetics and excretion studies of intravenously injected nanoparticles and extracellular vesicles: Possibilities and challenges. Adv Drug Deliv Rev, 2022. **186**: p. 114326.
- [8] VERBERNE H.J. et al., EANM procedural guidelines for radionuclide myocardial perfusion imaging with SPECT and SPECT/CT: 2015 revision. Eur J Nucl Med Mol Imaging, 2015. **42**(12): p. 1929-40.
- [9] SAHA G.B. *Fundamentals of Nuclear Pharmacy*. 2018, Springer International Publishing: Imprint: Springer,: Cham. p. 1 online resource, XVII, 428 pages 110 illustrations, 31 illustrations in color.
- [10] CARTER L.M. et al., The Impact of Positron Range on PET Resolution, Evaluated with Phantoms and PHITS Monte Carlo Simulations for Conventional and Non-conventional Radionuclides. Mol Imaging Biol, 2020. **22**(1): p. 73-84.
- [11] LOUDOS G., KAGADIS G.C., PSIMADAS D., *Current status and future perspectives of in vivo small animal imaging using radiolabelled nanoparticles*. Eur J Radiol, 2011. **78**(2): p. 287-95.
- [12] STOCKHOFE K. et al., Radiolabelling of Nanoparticles and Polymers for PET Imaging. Pharmaceuticals, 2014. **7**(4): p. 392-418.
- [13] KOLB H.C., FINN M.C., SHARPLESS K.B., Click Chemistry: Diverse Chemical Function from a Few Good Reactions. Angewandte Chemie International Edition, 2001. **40**(11): p. 2004-2021.
- [14] ZHAN Y. et al., Radiolabelled, Antibody-Conjugated Manganese Oxide Nanoparticles for Tumor Vasculature Targeted Positron Emission Tomography and Magnetic Resonance Imaging. ACS applied materials & interfaces, 2017. **9**(44): p. 38304-38312.
- [15] SATPATI D. et al., <sup>177</sup>Lu-labelled carbon nanospheres: a new entry in the field of targeted radionanomedicine. RSC Advances, 2016. **6**(56): p. 50761-50769.
- [16] MOON S.-H. et al., Development of a complementary PET/MR dual-modal imaging probe for targeting prostate-specific membrane antigen (PSMA). Nanomedicine: Nanotechnology, Biology and Medicine, 2016. **12**(4): p. 871-879.
- [17] TRUILLET C. et al., Synthesis and Characterization of <sup>89</sup>Zr-Labelled Ultrasmall Nanoparticles. Molecular Pharmaceutics, 2016. **13**(7): p. 2596-2601.
- [18] PIJEIRA M.S.O. et al., Radiolabelled nanomaterials for biomedical applications: radiopharmacy in the era of nanotechnology. EJNMMI Radiopharm Chem, 2022. **7**(1): p. 8.